

Synthesis and EPR Studies of Radicals and Biradical Anions of C₆₀ Nitroxide Derivatives

Francesca Arena,[†] Federico Bullo,[‡] Fosca Conti,[†] Carlo Corvaja,^{*†}
Michele Maggini,^{*‡} Maurizio Prato,[§] and Gianfranco Scorrano[‡]

Contribution from the Dipartimento di Chimica Fisica, Università di Padova, Via Loredan 2, I-35131 Padova, Italy, Centro Meccanismi di Reazioni Organiche del CNR, Dipartimento di Chimica Organica, Università di Padova, Via Marzolo 1, I-35131 Padova, Italy, and Dipartimento di Scienze Farmaceutiche, Università di Trieste, Piazzale Europa, 1, 34127 Trieste, Italy

Received July 29, 1996[⊗]

Abstract: A series of C₆₀ derivatives substituted with the nitroxide group 2,2,6,6-tetramethylpiperidine-1-oxyl have been synthesized. A detailed EPR and ENDOR study of the neutral radicals and of their reduction products is reported. All the neutral species give EPR spectra consisting of a main triplet of lines with ~15 G splitting by the ¹⁴N nucleus, typical of nitroxide radicals. Some of them show additional well-resolved splittings by methyl and methylene protons, which are discussed in relation to the conformation of the nitroxide ring. When the compounds are progressively reduced under vacuum by contact with an alkali metal mirror, new EPR lines are observed; a 1:1:1 triplet with a splitting constant half that of a nitroxide radical and $g = 2.0030$ is attributed to biradical anions where one electron is located in the fullerene moiety and experiences a strong exchange coupling with the nitroxide unpaired electron. Frozen solution spectra of these species allow the determination of the electron–electron dipolar interaction parameters which are compared with theoretical MO calculations. The experimental values agree with a spin distribution of one unpaired electron mostly in the equatorial plane of the fullerene. Another single line which appears in the spectrum as the reduction proceeds further on ($g = 1.9999$) is attributed to a new species: possibly a substituted fullerene radical anion in which the nitroxide group is irreversibly reduced.

Introduction

The C₆₀ fulleride anions have attracted a wide interest because of their connection with relevant fullerene properties, like the superconductivity of alkali-metal doped C₆₀¹ and the ferromagnetism of C₆₀(TDAE).²

C₆₀ⁿ⁻ anions ($n = 1, 2, 3$) have been prepared by a variety of chemical and electrochemical methods and they were characterized by near-IR, Raman, and EPR spectroscopies.^{3–6} In spite of the large number of studies on this subject, the elucidation of important features regarding the electronic structure of these species is still debated, such as, for example, the spin multiplicity of C₆₀²⁻. The magnetic susceptibility data of analytically pure C₆₀²⁻ salts⁷ indicate that C₆₀²⁻ is paramagnetic. The ground triplet and singlet states are very close in energy and are both thermally populated even at helium temperatures, in contrast with theoretical predictions⁸ and with pulsed EPR measurements.⁵

Recently we prepared a C₆₀ derivative having a nitroxide free radical substituent, and we investigated its excited quartet state. This could be described as arising from a triplet–doublet pair formed by triplet C₆₀ (³C₆₀), ferromagnetically coupled to the nitroxide electron spin doublet state.⁹

We reasoned that, because of its weak interaction, the nitroxide unpaired spin of fullerene–nitroxides could be useful also for studying C₆₀ anions, acting as a probe for their electronic distribution. A series of fullerene–nitroxide anions have been prepared by alkali metal reduction of the parent compounds **1–5** (Scheme 1) in 2-methyltetrahydrofuran (MeTHF). They display characteristic EPR spectra which are discussed in this paper. MeTHF was used as it forms, at low temperatures, a glassy matrix which allows the measurements of the anisotropy of the magnetic interactions.

Experimental Section

Instrumentation. EPR measurements were performed with a computer-controlled Bruker ER 200 DX-band EPR spectrometer, equipped with nitrogen flow temperature controller. The ENDOR spectra were recorded with the same spectrometer using a frequency modulated Rohde & Schwarz SMX RF signal generator and an ENI A-300 RF power amplifier. The ENDOR signal was feeded to a EG & G 5208 two phase lock-in analyser. A home-written software was used to control the RF sweep and the data acquisition. For g values calibration, the microwave frequency was measured by a 5342 A Hewlett-Packard microwave frequency counter and the magnetic field intensity by a G-502 Harvey-Wells NMR precision gaussmeter whose frequency was also monitored by the same frequency counter. MALDI (matrix-assisted laser desorption ionization) mass spectra were obtained

[†] Dipartimento di Chimica Fisica, Università di Padova.

[‡] Dipartimento di Chimica Organica, Università di Padova.

[§] Dipartimento di Scienze Farmaceutiche, Università di Trieste.

[⊗] Abstract published in *Advance ACS Abstracts*, December 15, 1996.

(1) Haddon, R. C. *Acc. Chem. Res.* **1992**, *25*, 127–133.

(2) Allemand, P.-M.; Khemani, K. C.; Koch, A.; Wudl, F.; Holczer, K.; Donovan, S.; Grüner, G.; Thompson, J. D. *Science* **1991**, *253*, 301–303.

(3) (a) Kato, T.; Kodama, T.; Oyama, M.; Okazaki, S.; Shida, T.; Nakagawa, T.; Matsui, Y.; Suzuki, S.; Shiramaru, H.; Yamauchi, K.; Achiba, Y. *Chem. Phys. Lett.* **1991**, *186*, 35–39. (b) Negri, F.; Orlandi, G.; Zerbetto, F. *J. Am. Chem. Soc.* **1992**, *114*, 2909–2913.

(4) Dubois, D.; Jones, M. T.; Kadish, K. M. *J. Am. Chem. Soc.* **1992**, *114*, 6446–6451 and references cited therein.

(5) Khaled, M. M.; Carlin, R. T.; Trulove, P. C.; Eaton, G. R.; Eaton, S. *J. Am. Chem. Soc.* **1994**, *116*, 3465–3474.

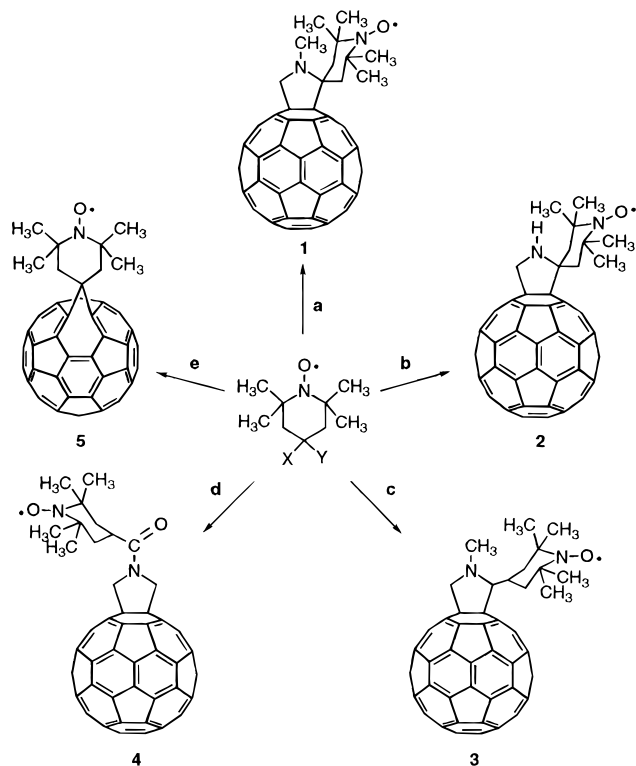
(6) Bhyrappa, P.; Paul, P.; Stinchcombe, J.; Boyd, P. D. W.; Reed, C. *J. Am. Chem. Soc.* **1993**, *115*, 11004–11005.

(7) Boyd, P. D. W.; Bhyrappa, P.; Paul, P.; Stinchcombe, J.; Bolskar, R. D.; Sun, Y.; Reed, C. A. *J. Am. Chem. Soc.* **1995**, *117*, 2907–2914.

(8) Negri, F.; Orlandi, G.; Zerbetto, F. *Chem. Phys. Lett.* **1988**, *144*, 31–37.

(9) Corvaja, C.; Maggini, M.; Prato, M.; Scorrano, G.; Venzin, M. *J. Am. Chem. Soc.* **1995**, *117*, 8857–8858.

Scheme 1



- a: X = Y = O; C₆₀, N-methylglycine, toluene, reflux, 7h, 13%.
 b: X = CO₂H, Y = NH₂; C₆₀·(CH₂O)_n, toluene, reflux, 30 min., 36%.
 c: X = H, Y = CHO; C₆₀, N-methylglycine, toluene, reflux, 2.5h, 14.6%.
 d: X = H, Y = CO₂H; N-H 3,4-fulleropyrrolidine, EDC/HOBt, CH₂Cl₂, 32%.
 e: X = Y = N₂, (ref. 14, 15)

in positive linear mode at 15 kV acceleration voltage on a mass spectrometer reflex time of flight (Bruker), using 2,5-dihydroxybenzoic acid as matrix. UV-vis absorption spectra were taken on a Perkin-Elmer Lambda 6 spectrophotometer. Reactions were monitored by thin-layer chromatography using Merck precoated silica gel 60-F₂₅₄ (0.25 mm thickness) plates. Flash column chromatography was performed employing 230–400 mesh silica gel (ICN Biomedicals). Reaction yields were not optimized and refer to pure, isolated products. The purity of all C₆₀ derivatives used in this work was checked by HPLC using a Primesphere silica column from Phenomenex (250 × 10 mm, 5 μm). Isocratic elution was performed on a LC pump unit Shimadzu LC-8A at a flow rate of 2 mL min⁻¹ with HPLC-grade toluene as the mobile phase. The elution was monitored with a Shimadzu SPD-6A UV spectrophotometric detector at 340 nm. The minimum-energy structures for fulleropyrrolidines 1–4 were calculated using the Spartan 3.1 program running on a IBM Risc/6000 250 workstation with the PM3 semiempirical method. EPR spectra simulations were performed by using the PIP program written by M. Nilges and provided by the Illinois EPR Research Center.

Materials. C₆₀ was purchased from Bucky USA (99.5%). All other reagents were used as purchased from Fluka and Aldrich. 4-Amino-4-carboxy-2,2,6,6-tetramethylpiperidine-1-oxyl (TOAC),¹⁰ 4-formyl-2,2,6,6-tetramethylpiperidine-1-oxyl (4-formyl-TEMPO),¹¹ tetramethyl-4-piperidone-1-oxyl (TEMPO),¹² unsubstituted N-H 3,4-fulleropyrrolidine,¹³ and fulleroid 5¹⁴ were prepared as described in the literature. All solvents were distilled prior to use. Methylene chloride and cyclohexane, employed for UV-vis measurements, were commercial spectrophotometric grade solvents.

(10) Dulog, L.; Wang, W. *Liebigs Ann. Chem.* **1992**, 301–303.

(11) Cseko, J.; Hankovszky, H. O.; Hideg, K. *Can. J. Chem.* **1985**, 63, 940–943.

(12) Dulog, L.; Seidemann, R. *Makromol. Chem.* **1986**, 187, 2545–2551.

(13) Prato, M.; Maggini, M.; Giacometti, C.; Scorrano, G.; Sandoná, G.; Farnia, G. *Tetrahedron* **1996**, 52, 5221–5234.

(14) Ishida, T.; Shinozuka, K.; Nogami, T.; Kubota, M.; Ohashi, M. *Tetrahedron* **1996**, 52, 5103–5112.

Synthesis of Fullerene Derivatives. The fullerene–nitroxides considered in this paper are shown in Scheme 1. Except for fulleroid 5¹⁵ (5,6-open, annulene-like structure), all compounds are 3,4-fulleropyrrolidines (FPNOs) in the form of the 6,6-closed isomer. Derivatives 1–3 have the 2,2,6,6-tetramethylpiperidine-1-oxyl moiety spiro linked (1 and 2) or linked (3) to position 2 of the pyrrolidine ring. They were prepared by reaction of the appropriate azomethine ylide precursor with C₆₀.¹⁶ N-Acylated derivative 4 was obtained by allowing N-H fulleropyrrolidine¹³ to react with 4-carboxy-2,2,6,6-tetramethylpiperidine-1-oxyl using 1-(3-(dimethylamino)propyl)-3-ethylcarbodiimide (EDC) and N-hydroxybenzotriazole (HOBt) as coupling agents.

N-Methyl-3,4-fulleropyrrolidine-2-spiro-4'-(2',2',6',6'-tetramethylpiperidine-1'-oxy) (1). A solution of 100 mg (0.14 mmol) of C₆₀, 97 mg (0.6 mmol) of TEMPO, and 87 mg (0.98 mmol) of N-methylglycine in 100 mL of toluene was stirred at reflux temperature for 7 h, and then the solvent was removed in vacuo. The residue was purified by flash column chromatography (eluent, toluene), affording 16 mg (13%) of 1 along with 80 mg (80%) of unreacted C₆₀. MALDI-MS C₇₁H₂₁N₂O (MW = 917): *m/z* 887 [(M – 2CH₃)⁺]. UV-Vis (CH₂Cl₂) λ_{max} (ε) 254 (84 261), 317 (39 203), 431 (3180). Anal. Calcd for C₇₁H₂₁N₂O: C, 92.89; H, 2.31; N, 3.05. Found: C, 93.33; H, 2.34; N, 2.94.

3,4-Fulleropyrrolidine-2-spiro-4'-(2',2',6',6'-tetramethylpiperidine-1'-oxy) (2). The synthesis was carried out as described for compound 1, starting from 310 mg (0.43 mmol) of C₆₀, 98 mg (0.46 mmol) of TOAC, and 60 mg (2 mmol) of paraformaldehyde in 300 mL of toluene. The reflux was prolonged for 30 min. Derivative 2: 140 mg (36%). Unreacted C₆₀: 168 mg (54%) MALDI-MS C₇₀H₁₉N₂O (MW = 903): *m/z* 904 [(M + H)⁺]. UV-Vis (CH₂Cl₂) λ_{max} (ε) 258 (145 750), 309 (54 300), 431 (7150). Anal. Calcd for C₇₀H₁₉N₂O: C, 93.00; H, 2.12; N, 3.10. Found: C, 92.91; H, 2.01; N, 2.94.

N-Methyl-3,4-fulleropyrrolidine-2-spiro-4'-(2',2',6',6'-tetramethylpiperidine-1'-oxy) (3). The synthesis was carried out as described for compound 1 using chlorobenzene as solvent, starting from 100 mg (0.14 mmol) of C₆₀, 27 mg (0.15 mmol) of 4-formyl-TEMPO, and 13 mg (0.15 mmol) of N-methylglycine dissolved in 100 mL of chlorobenzene. The reflux was prolonged for 2 h. Derivative 3: 19 mg (14.6%). Unreacted C₆₀: 78 mg (78%). MALDI-MS C₇₂H₂₃N₂O (MW = 931): *m/z* 932 [(M + H)⁺]. UV-Vis (CH₂Cl₂) λ_{max} 211, 256, 314, 431. Anal. Calcd for C₇₂H₂₃N₂O: C, 92.79; H, 2.49; N, 3.00. Found: C, 92.51; H, 2.40; N, 2.94.

N-(2',2',6',6'-tetramethylpiperidinyl-1'-oxy)carbonyl]-3,4-fulleropyrrolidine (4). A solution of 35 mg (0.18 mmol) of 4-carboxy-TEMPO, 24 mg (0.18 mmol) of N-hydroxybenzotriazole, and 34 mg of 1-(3-(dimethylamino)propyl)-3-ethylcarbodiimide hydrochloride (EDC·HCl) in 5 mL of CH₂Cl₂ was stirred at room temperature for 4 h. A solution of 3,4-fulleropyrrolidine, freshly prepared by treating 45 mg (0.049 mmol) of the corresponding ammonium trifluoromethane sulfonate salt¹³ with excess triethylamine (100 μL) in 5 mL of CH₂Cl₂ was added, and the mixture was stirred at room temperature for 4 days. The solvent was removed in vacuo and the residue purified by flash column chromatography (eluant, toluene/ethyl acetate, 1:1), affording 15 mg (32%) of 4. MALDI-MS C₇₂H₂₁N₂O₂ (MW = 945): *m/z* 946 [(M + H)⁺]. UV-Vis (CH₂Cl₂) λ_{max} (ε) 255 (130 433), 309 (40 358), 431 (3560). Anal. Calcd for C₇₂H₂₁N₂O₂: C, 91.42; H, 2.24; N, 2.96. Found: C, 91.00; H, 2.15; N, 2.77.

Anion Preparation. The radical anions of fullerene–nitroxides 1–5 (FNOs) were prepared by standard vacuum (ca. 10⁻⁴ mbar) techniques in a 10 mm o.d. Pyrex tube containing a few hundreds micrograms of FNO and in some cases FNO together with ether dibenzo-18-crown-6. The tube was equipped with two lateral arms, one being a usual EPR tube. In the second one a sodium or potassium mirror was formed by evaporating the pure metal before introducing the solvent through the vacuum line. After a few freeze–pump–thaw cycles, the apparatus was sealed.

The solution was carefully brought into contact with the metal mirror and the EPR spectrum was recorded after each contact.

(15) Ishida, T.; Shinozuka, K.; Kubota, M.; Ohashi, M.; Nogami, T. *J. Chem. Soc., Chem. Commun.* **1995**, 1841–1843.

(16) Maggini, M.; Scorrano, G.; Prato, M. *J. Am. Chem. Soc.* **1993**, 115, 9798–9799.

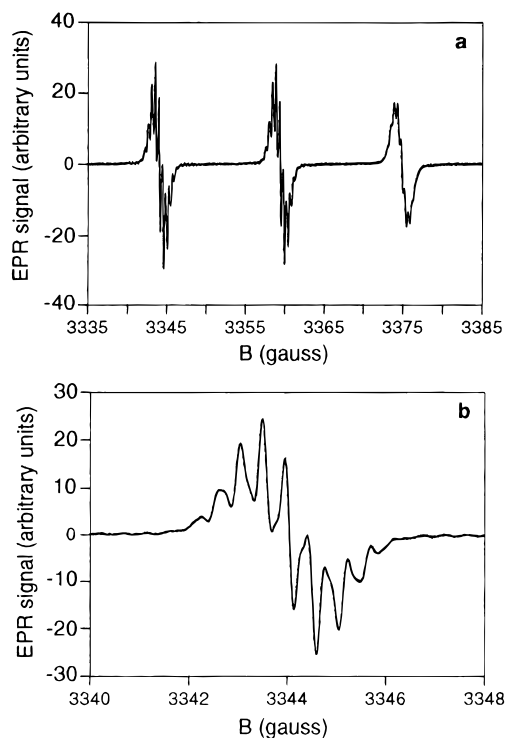


Figure 1. EPR spectra of fulleropyrrolidine **3** in MeTHF at room temperature. (a) The large splitting is due to the ¹⁴N hyperfine coupling while the further splittings are due to six protons of two axial CH₃ groups and two protons of CH₂ groups. (b) Low-field line of spectrum 1a.

Results

The EPR spectra of FPNOs **1–4** and of fulleroid **5** in MeTHF solution at room temperature consist of a triplet of lines of the same intensity deriving from the ¹⁴N hyperfine interaction. Further splittings by the protons of the methyl substituents and by the methylene protons of the piperidine ring are resolved for **3**, **4**, and **5**. Their spectra are characterized by narrow lines (peak to peak line widths < 200 mG). For **1** and **2** the line width is larger and no extra splittings are observed. A typical spectrum of compound **3** is shown in Figure 1. A low-resolution EPR spectrum of **5** in toluene was recently reported.¹⁵ This shows a much larger line width (2.3 G instead of 120 mG) probably due to the spectral broadening effect of oxygen in the solvent.

The proton hyperfine structure of derivative **3** can be analyzed in terms of hyperfine coupling of two (axial) methyl groups ($a_{\text{H}}^{\text{CH}_3} = 0.45$ G) and two methylene protons ($a_{\text{H}}^{\text{CH}_2} = 0.32$ G). Splittings are unresolved for the remaining protons. The hyperfine couplings were confirmed by ENDOR spectroscopy which shows, in addition to two lines due to ¹⁴N, two pairs of partially overlapped lines centered about the free proton frequency. The unequivalence of the axial and equatorial methyl protons and the value of their hyperfine coupling indicate a rigid structure of the nitroxide ring with chair conformation.¹⁷ This is in agreement with minimum energy structure calculations, performed on **3**, which are discussed later in this paper. The proton hyperfine structure of derivative **4** has been analyzed and indicates a rigid structure of the nitroxide unit as found for derivative **3**.

On the contrary, the proton hyperfine pattern of the EPR spectrum of **5** is consistent with splittings by two sets of 12 (four methyl groups) and of four (two CH₂ groups) protons. In this case the measured splitting constants, again obtained by

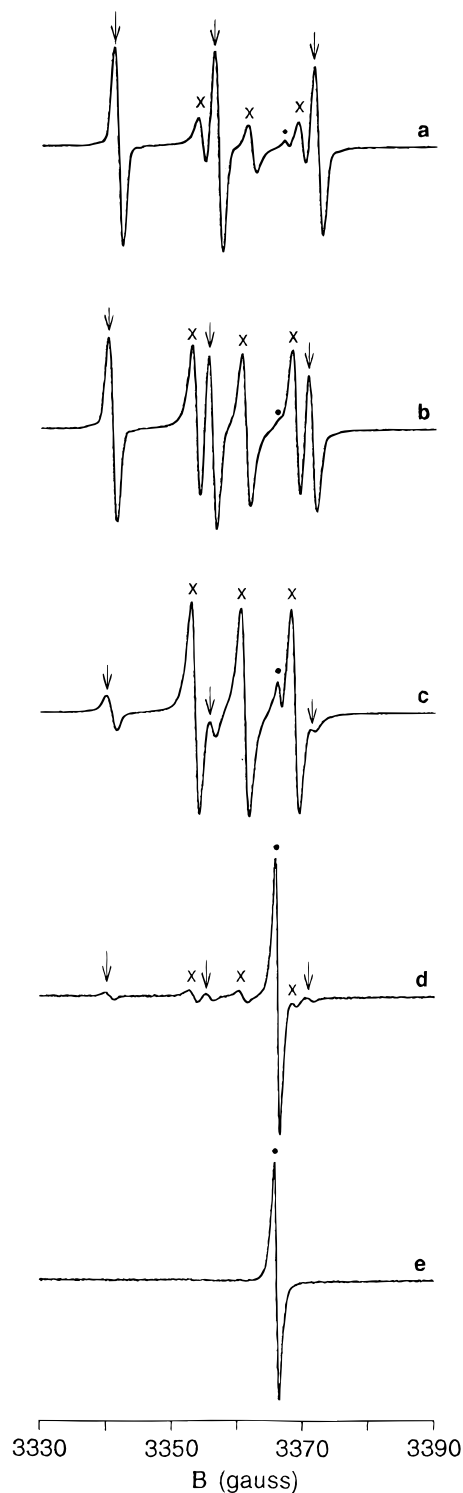


Figure 2. Room temperature EPR spectra of **1** (ca. 10⁻⁴ M) in MeTHF during the reduction process. The arrows indicate the hyperfine component of neutral **1**, separated by 15.3 G. Lines marked with crosses and separated by 7.65 G are due to the biradical anion of derivative **1**. The narrow line with low *g* factor (marked with a point) is due to a further reduction product which is the only one remaining after prolonged reduction (see text).

the best fitting of the ENDOR spectrum, are $a_{\text{H}}^{\text{CH}_3} = 0.21$ G and $a_{\text{H}}^{\text{CH}_2} = 0.17$ G, about half those of **3**. This is expected if the piperidineoxyl ring undergoes a fast conformation interconversion, which exchanges axial and equatorial groups.

As FPNOs **1–4** are progressively reduced by contact with the alkali metal mirror, the corresponding EPR spectrum changes and additional lines appear. The EPR spectrum of **1**, recorded

(17) Briere, R.; Lemaire, H.; Rassat, A.; Rey, P. *Bull. Soc. Chim. Fr.* **1967**, *12*, 4479–4484.

Table 1. *g* Factor and Hyperfine Splitting Constants (G)

compd	state ^a	<i>g</i>	<i>a</i>
1	n	2.0061	15.30
	ma	2.0030	7.65
	x	1.9999	
2	n	2.0061	15.15
	ma	2.0030	7.80
	x	1.9999	
3	n	2.0061	15.45
	ma	2.0030	7.83
	x	1.9999	
4	n	2.0061	15.38
	ma	2.0030	7.57
	x	1.9999	
5	n	2.0061	14.98
	ma		
	x	2.0001	

^a Notation: n, neutral FPNO; ma, FPNO monoanion; x, FPNO product of further reduction.

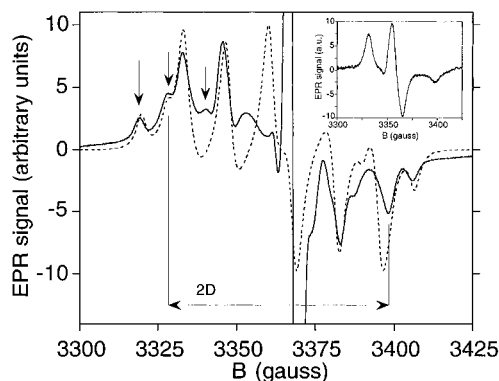


Figure 3. EPR spectrum of the reduction products of **3** in glassy matrix (MeTHF) at 120 K, and a computer simulation (dashed line). The arrows indicate the nitrogen splitting for the biradicals with the magnetic field parallel to the *z* component of the electron–electron dipolar tensor. Insert shows the frozen solution spectrum (*T* = 120 K) of the neutral starting material **3**.

after each contact of the solution with the alkali metal mirror, is shown in Figure 2. It consists of the superposition of lines due to three paramagnetic species having different *g* values and hyperfine splittings: a triplet (1:1:1 intensity ratio, *g* = 2.0061, *a_N* = 15.35 G, line width ΔB = 1.35 G) corresponding to the neutral fullerene nitroxide, a second triplet (1:1:1 intensity ratio, *g* = 2.0030, *a_N* = 7.65 G, ΔB = 1.35 G) attributed to the monoanion (vide infra), and a single narrower line (*g* = 1.9999, ΔB = 0.78 G) whose assignment is discussed later. As the reduction proceeds, the relative intensity of the single line at high field increases, and eventually the single line is the only one remaining after prolonged contact with the sodium or potassium mirror (Figure 2e).

In contrast to derivative **1** and to compounds **2–4** that show a similar behavior, fulleroid **5** does not show the anion three-line spectrum (vide infra for details). The *g* values and hyperfine splitting constants of the individual radicals are reported in Table 1.

Samples showing higher concentration of the monoanion, relative to the other species, were obtained by adding dibenzo-18-crown-6 in 1:1 stoichiometric ratio to the FPNO solution, before the contact with sodium or potassium.

The frozen solution spectra of these samples have a complex structure which is related to how the nitroxide unit is linked to the pyrrolidine ring. The EPR spectrum of the reduction products of **3**, shown in Figure 3, is used as reference for the discussion that follows. It could be computer simulated, as discussed in the next section, by assuming a random oriented

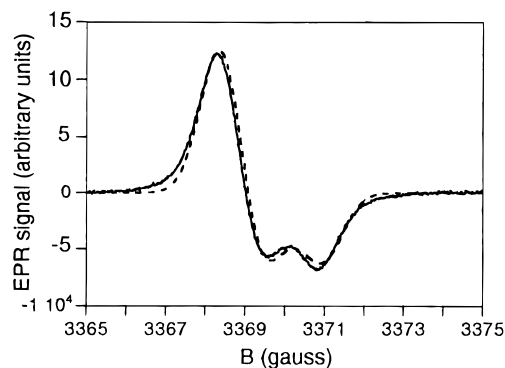


Figure 4. Single EPR line at low *g* value (see Figure 3) recorded at lower gain and modulation amplitude (solid line), and a computer simulation (dashed line) with the following set of *g* tensor components: (*g_{xx}* = 2.000 57, *g_{yy}* = 2.000 17, *g_{zz}* = 1.998 97).

collection of paramagnetic species having two unpaired electrons and a spin *I* = 1 nucleus. For comparison, the frozen solution spectrum of the neutral starting material **3** is shown in the inset.

The narrow single line of the fully reduced FPNO in the low-temperature MeTHF glassy matrix shows the typical shape due to the anisotropy of the *g* tensor.⁶ It could be computer-simulated assuming a *g* tensor with three different principal values (rhombic symmetry). The following set of values: *g_{xx}* = 2.000 57, *g_{yy}* = 2.000 17, *g_{zz}* = 1.998 97 fits quite well the spectrum recorded for **3** (Figure 4).

Discussion

Neutral FNOs. All neutral species **1–5** give EPR spectra consisting of a main triplet with splitting in the range 14.98–15.45 G. The splitting due to the ¹⁴N nucleus is typical of nitroxide radicals and reflects the immediate environment of the NO group. A point of interest is the fact that the three nitrogen hyperfine components show a broadening patterns with a pronounced linear dependence on the ¹⁴N nuclear spin component *m_I*. This broadening, which is much more evident in the spectra recorded at low temperature, is due to a strong anisotropy of the rotational diffusion tensor. This feature has been already discussed in earlier work.⁹

The proton hyperfine patterns of the EPR spectra of **3** and **4** could be computer simulated, assuming splittings by two sets of six (two methyl) and two (methylene) protons. The splitting by the other protons is not resolved.

The observation that only one pair of methyl groups contributes to the proton hyperfine splitting is a clear indication that the conformation of the nitroxide ring is rigid. Moreover, the couplings agree with a chair conformation.¹⁸ A possible conformational interconversion takes place at a rate much lower than the difference of the axial and equatorial hyperfine couplings in frequency units and the upper limit is on the order of a few hundreds kilohertz.

On the contrary, the proton splittings for **5** by four equivalent methyl groups indicate a fast conformation interconversion.

The nitroxide radical does not contain a net electronic charge and its conformation is expected not to be affected by the addition of one or two electrons in the molecule, provided they enter in the fullerene moiety, as will be shown to be the case. For that reason we assume that the same rigid conformation of the nitroxide ring is maintained also in the anionic species.

FNO Anions. The lowest unoccupied energy level of the highly symmetric C₆₀ molecule is 3-fold degenerate and can accommodate up to six electrons. Accordingly, up to six

reversible reduction peaks have been observed by cyclic voltammetry (CV) of C₆₀ in oxygen free aprotic solvents.^{19,20} In the anionic species, Jahn–Teller instability is expected to decrease the symmetry.³ Lower symmetry is also produced in solvents of low dielectric constant by the presence of the counterion. Different types of distortions have been considered, giving rise to structures having *D*_{5d}, *D*_{3d}, or *D*_{2h} symmetry.²¹ Ab initio calculations have shown that these structures have similar energies.²¹ In the *D*_{2h} structure the LUMO belongs to the b_{1u} symmetry species and presents a node at the 6,6-ring junction which is perpendicular to the 2-fold symmetry axis.

In fulleropyrrolidines with no substituents in positions 2 and 5 of the pyrrolidine ring (e.g. *N*-methylfulleropyrrolidine) the 3-fold degeneracy of the C₆₀ LUMO is lifted by the substitution as these molecules have approximately *C*_{2v} symmetry. Moreover, since the pyrrolidine ring is fused to a 6,6-ring junction of C₆₀ on the nodal position, the effects on the LUMO properties of the *D*_{2h} distorted C₆₀ moiety should be of minor importance. In particular, the symmetry plane perpendicular to the 2-fold symmetry axis is retained. Semiempirical calculations, using PM3 method, confirm this expectation. A similar situation occurs also in other dihydrofullerenes.²² Substitution in position 2 of the pyrrolidine ring (compounds **1–4**) does not affect the LUMO properties as well.

The cyclic voltammetry curves of FPNO **1–4** (5 × 10^{−4} M) in THF at room temperature, on a Pt electrode, using tetrabutylammonium hexafluorophosphate (5 × 10^{−2} M) as supporting electrolyte, show five reversible reduction peaks for the fullerene and one irreversible reduction process due to the nitroxide substituent, positioned between the third and fourth fullerene moiety reduction steps. On the oxidation side, the reversible oxidation of the nitroxide is observed. The values of the reduction potentials of FPNOs **1–4** are similar to those found for other fulleropyrrolidines.¹³ For example, the reduction potentials *E*⁰ of **2** in volts vs Fc⁺/Fc are −0.99, −1.55, −1.95, −2.17, and −2.64. The reduction peak at −1.95 V together with an oxidation peak at +0.32 V refers to processes involving the nitroxide group.²³ This finding supports the assumption of a minor substituent effect on the LUMO energy and the view that the added electron of the anion resides on the fullerene moiety. In the cyclic voltammetry curve of fulleroid **5**, taken at slow potential scan rate and at room temperature, the first reduction process is irreversible. This probably precludes the observation of the anion three-lines spectrum during chemical reduction. Further investigation on the EPR behavior of **5** is beyond the scope of this work.

FPNO monoanions have two unpaired electrons and therefore have a singlet and a triplet electronic states. Because of the relatively large distance between the two spin distributions, one being localized on the nitroxide group, the exchange interaction, which separates the energies of the triplet and the singlet states, is expected to be in the order of a fraction of a cm^{−1}. Therefore at room temperature both states should be almost equally populated and FPNO monoanions should be considered as biradicals.

Several symmetrical bis-nitroxide biradicals have been reported,²⁴ and their EPR spectrum was described to the first

order by the spin hamiltonian:

$$H = g\beta B_0(S_{1z} + S_{2z}) + a_N(S_{1z}I_{1z} + S_{2z}I_{2z}) + J(S_1 \cdot S_2) \quad (1)$$

where *S*_{1z} and *S*_{2z} are the *z* spin components of the two unpaired electrons and *I*_{1z} and *I*_{2z} are the nuclear spin components of the two ¹⁴N nuclei, which are assumed to have the same hyperfine coupling *a*_N.

The presence of the exchange interaction term *J*(*S*₁·*S*₂) has dramatic effects on the EPR spectrum. If *J* is much larger than the ¹⁴N hyperfine coupling *a*_N, the splitting constant is predicted to be *a*_N/2, one-half the coupling constant for a nitroxide monoradical.^{24,25} At the same time the number of lines becomes five (1:2:3:2:1 intensity ratios) instead of three (1:1:1) because each unpaired electron interacts with the ¹⁴N nuclei of both nitroxide moieties.

FPNO monoanions are biradicals containing a single nitroxide and only one ¹⁴N-coupled nucleus. Therefore, in the case of *J* ≫ *a*_N, a hyperfine splitting constant *a*_N/2 should be observed, but still with a three-line splitting. This is indeed the case in the monoanion spectrum; the experimental values of the splitting constants reported in Table 1 are within the experimental errors one-half those of the neutral FPNOs. It is interesting to note that condition *J* ≫ *a*_N is verified also for **4** where the nitroxide is relatively far from the fullerene.

A second effect of the exchange interaction is the averaging of the *g* factor values corresponding to two limiting cases: the whole unpaired electron distribution only on the fullerene and the unpaired electron localized on the nitroxide radical. In fact the experimental value (*g* = 2.0030) corresponds to the average value between *g* of the *N*-methylfulleropyrrolidine monoanion (*g* = 1.9998)²⁶ and *g* of the nitroxide free radical FPNO (*g* = 2.0061).

In the low-temperature MeTHF rigid glass matrix the electron–electron and the electron–nucleus dipolar interactions are no longer averaged out and the dipolar interaction terms of the spin hamiltonian should be taken into account. The dipolar interactions are described by the spin hamiltonian:

$$H_d = S \cdot \mathbf{D} \cdot S' + S' \cdot \mathbf{T}_{\text{nit}} \cdot I_N + S \cdot \mathbf{T}_{\text{ful}} \cdot I_N \quad (2)$$

S and *S'* are the unpaired electron spin on the fullerene and on the NO group respectively, *I*_N the nitroxide ¹⁴N nuclear spin. **D** is the electron–electron dipolar tensor while **T**_{nit} and **T**_{ful} are respectively the hyperfine dipolar tensors contributions coming from the spin densities of *S'* on the nitroxide and of *S* on the fullerene moiety. Because of the large distance of the latter from the location of the nitrogen nucleus, the last term can be neglected.

A computer simulation of the EPR spectrum is shown in Figure 3 (dashed line). It was obtained assuming a random orientation distribution of paramagnetic species with the spin hamiltonian (2) added to the Zeeman and exchange terms. It should be noted that the principal axes of the three tensors **D**, **T**, and **g** do not coincide. This fact complicates the computer simulation of the experimental spectrum. However, the field values for the absorption peaks were satisfactory reproduced with the magnetic parameters reported in Table 2. *A*_{zz} represents the hyperfine splitting for those radicals oriented with the

(19) Xie, Q.; Pérez-Cordero, E.; Echegoyen, L. *J. Am. Chem. Soc.* **1992**, *114*, 3978–3980.

(20) Ohsawa, Y.; Saji, T. *J. Chem. Soc., Chem. Commun.* **1992**, 781–782 and references quoted therein.

(21) Koga, N.; Morokuma, K. *Chem. Phys. Lett.* **1992**, *196*, 191–196.

(22) Hirsch, A.; Lamparth, I.; Grösser, T. *J. Am. Chem. Soc.* **1994**, *116*, 9385–9386.

(23) Paolucci, F.; Roffia, S. Personal communication. We thank Dr. F. Paolucci and Prof. S. Roffia (Università di Bologna, Italy) for disclosing to us some of their unpublished results.

(24) Luckhurst, G. R. Biradicals as Spin Probes. In *Spin Labeling, Theory and Applications*; Berliner, L. J., Ed.; Academic: New York, 1976; Chapter 4, pp 133–181.

(25) Rozantsev, E. G. *Free Nitroxyl Radicals*; Plenum: New York, 1970.

(26) Brustolon, M.; Zoleo, A. Personal communication. We thank Prof. M. Brustolon and Dr. A. Zoleo (Università di Padova, Italy) for disclosing to us some of their unpublished results.

Table 2. Zero Field Splitting Parameters and Hyperfine Splitting Constant^{a,b}

species	<i>D</i>	<i>E</i>	<i>A_{zz}</i>
1	41	0	9
	(42)	(1)	(-)
3	35	0	9
	(40)	(1)	(-)

^a Restricted HF calculation given in parentheses. ^b All the values are in gauss.

magnetic field directed along the principal axis *z* of the electron–electron dipolar interaction.

The fact that details of the spectrum shape are not fully accounted for could be due to several reasons. For example, the spectrum intensity may include contributions due to the presence of the neutral radical (see the inset in Figure 3) in addition to the species responsible for the intense single line. Moreover, residual motion of the molecule in the glassy matrix had to be taken in account. These effects were not included in the simulation.

It is interesting to note that the values used in the simulation for the hyperfine tensor agree with those obtained by single crystal EPR²⁷ and ENDOR²⁸ studies on nitroxides. Of course these values are scaled by a factor of 2 because of the exchange interaction, which we know is much larger than the isotropic ¹⁴N coupling.

The value for *D* and *E* will be compared with those expected for different spin distributions.

In order to calculate the dipolar interaction tensor the spin distribution on the fullerene moiety is needed. Several authors have considered the problem of the spin distribution in C₆₀⁻ radical anion. Koga and Morokuma performed ab initio unrestricted Hartree–Fock (UHF) calculations under the constraints of a symmetry lower than that of the neutral C₆₀ (*I_h*) as predicted by the Jahn–Teller theory. In particular they considered *D*_{5d}, *D*_{3d}, and *D*_{2h} symmetries.²¹ The latter is the appropriate one for 1,2-disubstituted fullerenes on a 6,6-ring junction. Unfortunately we cannot use their results for the spin densities because UHF method gives molecular wave functions contaminated by terms of higher multiplicities. Even though the contamination is not too large for affecting the calculated energies of the Jahn–Teller distorted structures, it is quite disturbing for the spin densities. In fact the reported data sum up to a total of 1.6 which would not be appropriate for our purpose of evaluating the dipolar interaction with the nitroxide electron spin.

Because of this difficulty, we considered the spin distribution in the fullerene as it results from a (restricted) HF calculation on the neutral *N*-methylfulleropyrrolidine by taking the squares of the LUMO coefficients. On the other hand, it was emphasized that addition of a single electron to a large system changes only slightly the electron distribution.⁸

It turns out that the spin distribution is mostly confined on the equatorial belt of C₆₀ (Figure 5). About 50% of the total spin density is located on the 12 atomic positions indicated by black circles. Up to 68% of the total spin density is accounted for by adding the other eight atomic positions (gray circles).

The geometry of the FPNO, which is necessary for localizing of the nitroxide electron spin, is taken from minimum energy molecular structure semiempirical PM3 calculations. Finally the dipole–dipole interaction was calculated with the point dipole approximation, justified by the large distance between the two electrons.

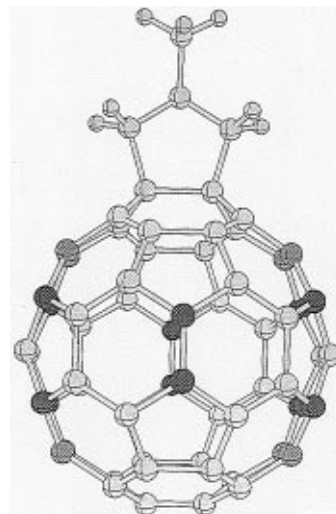


Figure 5. Atomic positions with the highest spin densities in the *N*-methylfulleropyrrolidine anion. About 50% of the total density is located on the 12 atoms represented by black circles; up to 68% is accounted for by adding the eight atoms represented by gray circles.

The results concerning the dipolar interaction tensor are reported in Table 2. The good agreement between the data obtained from the EPR spectrum and the values obtained by the HF spin distribution calculation could be considered as an “experimental” confirmation that the distribution of the unpaired electron in the fullerene derivative monoanion is mainly on the equatorial plane. Calculations performed by assuming a spin density distribution located at the fullerene polar regions give **D** tensor values much larger than the experimental ones.

The Single Line at *g* = 1.9999. The nature of the species responsible for the single line at *g* = 1.9999 is not a simple question.

According to the reversibility of the first two reduction steps of FPNOs, we should expect the further reduction of FPNO anions to produce the dinegative ions. Since nitroxide radicals can be reduced (irreversibly) at more negative potentials than the second reduction potential of the FPNO, it is reasonable to consider that also the second electron added to the FPNO to form the dianion is localized mainly on the fullerene C₆₀ moiety. For this reason, FPNO²⁻ should be considered as nitroxide-labeled C₆₀²⁻.

There has been a debate on the question whether C₆₀²⁻ is paramagnetic or not.^{5,7} Recent EPR and magnetic susceptibility measurements favor the second hypothesis.⁷

The presence of two unpaired electron spins on the fullerene moiety in FPNO dianions is quite unexpected because the degeneracy of LUMO orbitals of C₆₀ is removed in fulleropyrrolidines.

For C₆₀²⁻ moiety of the nitroxide-labeled fulleropyrrolidine in the singlet state, one expects an EPR spectrum typical of a nitroxide radical with three lines separated by approximately 15 G as for the neutral FPNO. However, further reduction of the FPNO monoanion does not give rise to a new three-line spectrum; neither do we observe an increase of the signal intensity of the lines in the position corresponding to the neutral species. The latter should have been the case if the nitrogen coupling constants of neutral radical and dinegative ions were the same. On the contrary, we observe that the single line at 1.9999 increases.

A possible candidate for this line is the negative ion of a species derived from FPNO in which the nitroxide has been irreversibly reduced. This fulleropyrrolidine derivative should be reduced to the radical anion at the potential of the first

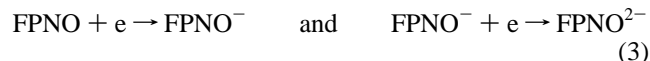
(27) Griffith, O. H.; Cornell, D. W.; McConnell, H. M. *J. Chem. Phys.* **1965**, *43*, 2909–2910.

(28) Brustolon, M.; Maniero, A. L.; Corvaja, C. *Mol. Phys.* **1984**, *51*, 1269–1281.

reduction peak of FPNO or very close to it. An argument in favor of irreversible reduction of the nitroxyl is the well-known fact that potassium is a strong enough reducing agent to reduce nitroxyls. The *g* factor value (*g* = 1.9999), which practically coincides with that of *N*-methylfulleropyrrolidine anion (*g* = 1.9998),²⁶ further supports this hypothesis. A higher value is expected for the dianion being the *g* factor of C₆₀²⁻ 2.0010.

In order to assign the single line to a FPNO dianion, one should justify the absence of any hyperfine structure in the EPR spectrum.

Furthermore, according to cyclic voltammetry measurements, carried out in THF with tetrabutylammonium hexafluorophosphate as supporting electrolyte, the potentials of the redox processes



are separated by 500 mV. From this value, one obtains for the disproportionation equilibrium



a constant $K_{\text{eq}} = 4 \times 10^{-10}$ which is not compatible with the presence of neutral, monoanion, and dianion species in comparable concentration, as observed.

Finally, it is interesting to note that if oxygen is admitted to the fully reduced solution, the original spectrum of the neutral nitroxide species is recovered.

Conclusion

Fulleropyrrolidines having a nitroxide unit can be reduced by alkali metals to biradical anions where one electron spin is localized on the nitroxide group and the second one is located on the fullerene moiety. The EPR spectra of these species,

consisting of a 1:1:1 triplet with splitting constant one-half that of a typical nitroxide free radical, indicate a strong exchange coupling between the two electrons. Also, the *g* factor corresponds as expected to the mean of the values for a nitroxide and a fulleropyrrolidine anion.

The magnetic dipolar interaction between the two electron spins is consistent with a spin distribution on the C₆₀ moiety mostly confined in the equatorial belt. Such spin distribution is predicted for the anion radical of C₆₀ after Jahn–Teller distortion along one of the 2-fold symmetry axes. This fact supports the idea that saturation of a double bond in C₆₀ does not affect the *t*_{1u} LUMO properties for this *D*_{2h} distorted structure. The electron distribution inferred by EPR experiments seems to agree with that obtained by Reed²⁹ based on the geometry of the dianion and interpreted in terms of the nodal structure of the *t*_{1u} orbital.

The single line, which is present in the EPR spectra of FPNOs solutions after prolonged contact with the alkali metal mirror, is probably due to the radical anion of a new species where the nitroxide group is irreversibly reduced.

The use of a nitroxide substituent as an external spin probe constitutes a valuable tool for the investigation of the electronic structure of fulleropyrrolidines.

Acknowledgment. This work was supported in part by the Italian National Research Council (CNR) through the Centro Studi sugli Stati Molecolari Radicalici ed Eccitati and Progetto Strategico Materiali Innovativi and by the Ministero dell'Università e della Ricerca Scientifica e Tecnologica (MURST). The authors thank Dr. R. Seraglia (CNR, Padova, Italy) for MALDI-MS data and Dr. M. Nilges (Illinois EPR Research Center) for the PIP simulation program.

JA9626291

(29) Paul, P.; Xie, Z.; Bau, R.; Boyd, P. D. W.; Reed, C. A. *J. Am. Chem. Soc.* **1994**, *116*, 4145–4146.